POLITECNICO DI TORINO
Repository ISTITUZIONALE

A Distributed Equivalent-Permeability Model for the 3-D Design Optimization of Bulk Superconducting Electromechanical Systems

Terms of use:

(Article begins on next page)

02 September 2025

A Distributed Equivalent-Permeability Model for the 3D Design Optimization of Bulk Superconducting Electromechanical Systems

Inês S.P. Peixoto, *Student Member, IEEE,* F. Ferreira da Silva, João F. P. Fernandes *Member, IEEE,*
Silvio Vaschetto *Senior Member, IEEE* and P. J. Costa Branco *Member, IEEE*

Abstract—This paper deals with accelerating 3D optimization scenarios for bulk superconductor-based electromechanical systems. For this objective, distributed equivalent-permeability models for High-Temperature-Superconducting bulks are first developed. These are stationary models capable of replicating the distribution of electromagnetic forces in bulks when subjected to external magnetic fields, minimizing the need for time-dependent simulations using the E-J power law. After introducing these models, their initialization phases are proposed to minimize their computational time requirements while still providing good accuracy. Optimization of a 3D Zero-Field-Cooled levitation system is presented to demonstrate the models' applicability. To validate the equivalent-permeability model, experimental tests are carried out. The measured experimental levitation forces resulting close to the ones obtained using the proposed equivalent-permeability model and the time-dependent $H-$formulation with the E-J power law. After validation, a multi-objective optimization using the NSGA-II tool is performed to maximize levitation force while minimizing the HTS bulk volume. Hence, using the equivalent-permeability models, stationary and linear FEM simulations provide highly accurate results and significantly reduce computational time, mainly in 3D optimization scenarios.

Index Terms—Equivalent models, Electromagnetic Force Computation, FEM Models, Geometric optimization, High-Temperature-Superconductors, Superconducting Bulk.

I. INTRODUCTION

WITH High-Temperature-Superconducting (HTS) technology is becoming more accessible, and new opportunities for HTS applications are emerging. Several applications are currently being studied in renewable energy generation, tackling surging concerns with pollution and sustainable development [1], [2]. In electrical machinery, these have been studied for in induction [3], [4] and synchronous motors [5],

[6], as well as for transportation systems, particularly for ship propulsion [7], [8] and aircraft applications [9], [10]. Superconductor applications in these areas have the potential to provide higher efficiency and specific power/torque when compared to conventional materials.

The first step in developing bulk superconductor-based devices is their electromechanical and thermal design, including their design optimization. This design phase usually requires extensive simulation through computational methods such as Finite Element Models (FEMs). The majority of FEM simulations used for computation of volume distribution of magnetization vector in bulk superconductors use the E-J power law together with an $H-$formulation [11]–[13] or an A-formulation [14], [15]. These simulations provide highly accurate results but are usually time-consuming, especially when dealing with 3D simulations with the highly non-linear characteristic of HTS materials, and also due to the great detail that is imperative for precise results [16]. In the case of optimization processes containing complex devices with HTS bulks, the high computational times of these methods are especially critical, considering that several thousands of simulations are usually required. Recent studies show that a combination of two formulations, one for non-linear conductive regions (e.g., HTS bulks), and another for non-conductive regions (e.g., air), provides the same results with lower simulation times [16], [17]. This is the example of the $H-\phi$ formulation, which can reduce about half the computational time required compared with $H-$formulation [18]. However, supposing these FEM simulations are being used to compute the electromagnetic forces distribution inside the HTS bulk for optimization purposes. In that case, simulation times are still very high to be incorporated in the optimization design stage. One example is the optimization done in [16], where the magnetization of an HTS bulk is simulated in 3D using the $H-\phi$ formulation, which still requires about 30 min for one simulation only.

When the electromagnetic force optimization is performed by considering different geometric configurations, such as the dimensions of HTS bulks and Permanent Magnets (PMs) in Maglev systems or even the relative position between them, and having FEM simulations taking about 30 minutes to complete, large-scale multi-variable optimizations are infeasible, time-wise. For this reason, new faster models are required to

reduce the highly time-consuming design phase in HTS bulk devices, even at lower accuracy.

According to the research developed in [19], a new model using an equivalent magnetic permeability for the HTS bulk can quickly estimate the levitation forces on it. The importance of this model lies in the electromagnetic characterization of the full HTS bulk by an equivalent magnetic permeability, which value changes with the applied magnetic field. The methodology assures the same magnetic energy stored in the bulk to the value obtained when simulating using the E-J power law. In short, the model allows the simulation of the HTS bulk using stationary studies instead of time-dependent ones. Even though the model does not provide results as precise as with $H-$formulation, it allows us to quickly obtain the optimal geometric configuration based on a straightforward initialization of the equivalent-permeability model. Therefore, its critical merit lies in its application for large-scale systems with multiple bulk samples and other materials. This equivalent magnetic permeability was already verified and applied for the optimization of a horizontal axis HTS ZFC levitation bearing with multiple HTS bulks on the stator and PM rings on the rotor [19].

When initialized, the equivalent-permeability model results are sufficiently accurate to be used in the force calculation of bulk superconductor-based devices. As such, optimization algorithms can now be performed using stationary studies with very short computational times, as initially shown in [19]. Pursuing this method, a variable spatial distribution of the equivalent magnetic permeability was also proposed throughout volume discretization of the HTS bulk for application on a previously developed cylindrical Maglev device [20]–[22]. Research in [20] performs an analysis of the most efficient volume sectioning of the HTS bulk while providing an analysis of the relative error for force computation between the equivalent model and the time-dependent E-J power law model for different air gap distances between the PM and the bulk.

Following that research, this paper focuses on applying and validating the distributed equivalent-permeability model now with the most accurate volume sectioning method in optimizing a 3D Zero-Field-Cooled (ZFC) levitation system. In addition, a novel methodology for initializing the equivalent-permeability model is proposed, greatly reducing the computational time by decreasing the number of required initializing simulations. The equivalent model is thus tested by performing a large-scale geometric and multi-objective optimization on superconductor bulks for force maximization and volume minimization. Furthermore, experimental tests measuring the levitation forces are carried out to validate the optimized solution. The method's accuracy is then evaluated based on the proximity between the configuration (geometrical variables) that allows force maximization and volume minimization found through the equivalent models and those achieved using the E-J power law model.

This paper is divided into six sections. In section II, the equivalent-permeability model concept is presented. In section III, the proposed application method of the distributed equivalent-permeability model is developed. In section IV, the
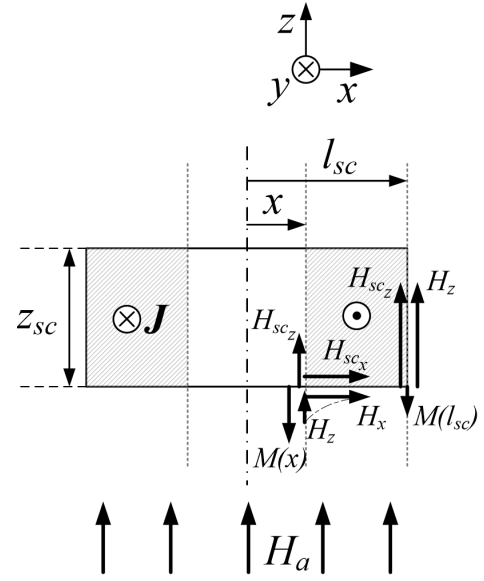
Fig. 1. Generation of the magnetization field M that according to the magnetic field boundary conditions causes deflection of the magnetic field lines in the region nearby the superconductor [19].

proposed initialization process of the model is presented and discussed. In section V, experimental results are shown to validate the proposed model and the initialization processes, and in section VI, a multi-objective optimization of the 3D levitation system is presented.

II. EQUIVALENT-PERMEABILITY MODEL CONCEPT

This section comprises the theoretical basis for the equivalent-permeability model. Consider, in Fig. 1, a rectangular bulk superconductor aligned with the $z-$axis under a uniform applied magnetic field $\mathbf{H_a} = \frac{B_a}{\mu_0}\mathbf{e_z}$. It is assumed that the bulk is surrounded by air. Hence the magnetic permeability of the cryocooling environment and the superconductor domain is μ_0.

From a macroscopic point of view, if the applied magnetic flux varies in time, an electric field $\mathbf{E}$ is induced inside the superconductor, according to Faraday's law. The induced current density $\mathbf{J} = J\mathbf{e_y}$, inside the SC along the $z-$axis, creates a magnetization field $\mathbf{M}$ as stated by (1).

$$\nabla \times \mathbf{M} = \mathbf{J} \tag{1}$$

Here, considering the direction of the current stays

$$\mathbf{M} = -M\mathbf{e_z} + M\mathbf{e_x} \tag{2}$$

This field causes deflection of the magnetic field lines in the region close to the superconductor. This resulting field will have components along the x-axis and z-axis, H_x and H_z, shown in Fig. 1. The magnetic field penetrating the SC can be written as,

$$\mathbf{H_{sc}} = H_{sc_z}\mathbf{e_z} + H_{sc_x}\mathbf{e_x} \tag{3}$$

because there is continuity of the magnetic flux density both in the longitudinal and tangential directions [19]. The resulting field's component in the longitudinal direction at the top and bottom boundaries of the SC is defined by

$$\mathbf{H_z} = (H_a - M)\mathbf{e_z} \tag{4}$$

Therefore, the relative equivalent-permeability of the superconductor medium after its magnetization [19] can be defined by

$$\mu_{eq} = \frac{||\mathbf{H_{sc}}||}{||\mathbf{H_a}||} = 1 + \frac{B_M}{B_a} = 1 + \chi \tag{5}$$

where $B_M = \mu_0 M$ and χ is the magnetization coefficient.

In the context of levitation systems, it has been demonstrated that the primary magnetic field component within the superconductor is oriented perpendicular to the applied field direction, specifically H_{sc_x}. This is supported by the observation that levitation forces exhibit considerably higher amplitudes than guidance forces [19]. Given that the present analysis pertains to the levitation forces in ZFC-based systems, it suffices to consider solely the field norm component to compute an isotropic permeability value, as opposed to the individual field components along the x- and z-axes. It should be noted, however, that this model is not suitable for large lateral motion due to its reliance on the magnetic field norm and the fact that the system generates mostly levitation forces.

III. USING THE DISTRIBUTED EQUIVALENT-PERMEABILITY MODEL

As seen in the previous section, the equivalent-permeability model requires an initialization based on the knowledge of the magnetic field distribution inside the superconductor volume when a magnetic field is applied. This initialization is an important step to reduce the uncertainty of the model and can be computed a priori for a set of applied magnetic fields. After the initialization, the distributed equivalent-permeability model can be employed to optimize bulk superconductor-based devices using stationary simulations.

A. The 3D Zero-Field-Cooled Levitation System

In this work, the optimization of a 3D Zero-Field-Cooling levitation component shown in Fig.2(a) is evaluated using multi-objective optimizations based on distributed equivalent-permeability model. The system is composed of a YBCO bulk above a permanent magnet. The permanent magnet geometry was set as a bulk with variable parameters x_{PM} and y_{PM}, as shown in Fig. 2(a), and z_{PM} that has a fixed value during the optimization due to its negligible effect in force levitation. Table I lists the range of each PM/SC geometric variable and Table II the YBCO and PM parameters.

For validation of the distributed equivalent-permeability model and its initialization process, 3D FEM simulations and experimental results were carried out. The 3D FEM simulations consisted of time-dependent $H - A$ formulation, employing the H-formulation with the E-J power law for the SC bulks, and the A-formulation for the remaining domains. The ZFC magnetization of the HTS bulks, i.e., applied magnetic field H_a, is performed by applying a smooth step
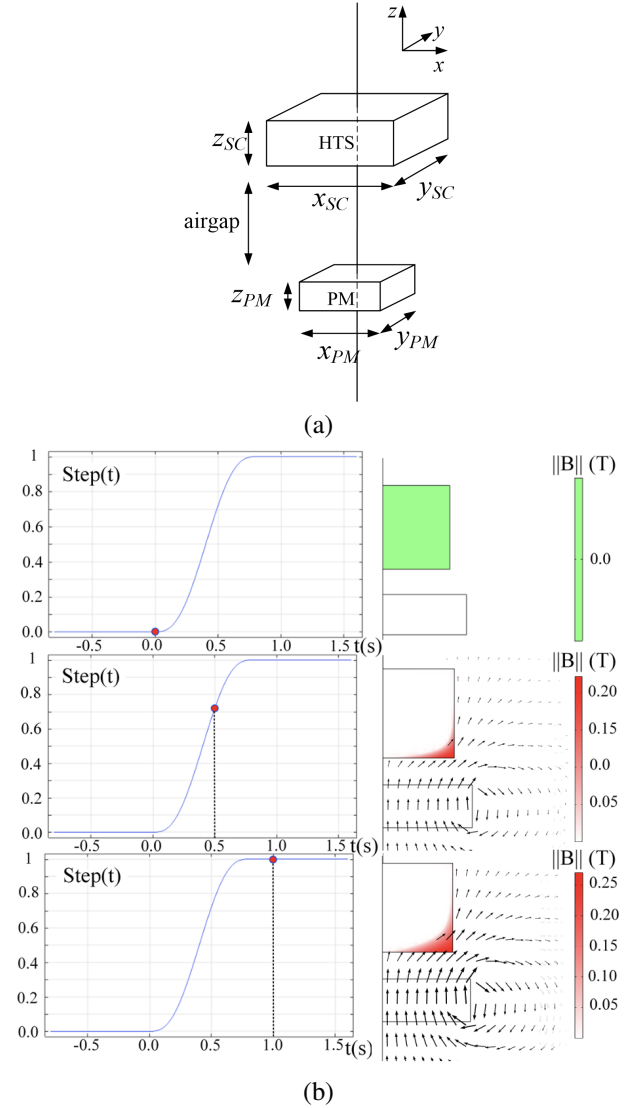
Fig. 2. (a) 3D view of SC and PM, their dimension variables, and associated coordinate axis. (b) Step function and magnetic field application. Each blue dot in the left images marks the time frame in which the right field images were taken. Arrow surface - B_x and B_z components; Surface - field norm $||\mathbf{B}||$.

TABLE I
GEOMETRIC PARAMETERS FOR THE VARIABLE SUPERCONDUCTOR AND PM PARAMETRIC SWEEP ([MIN VALUE: STEPS: MAX VALUE]).

x_{SC}(cm)	y_{SC}(cm)	z_{SC}(cm)
[1.6 : 1.2 : 6.4]	[1.6 : 1.2 : 6.4]	[0.7 : 0.525 : 2.8]
x_{PM}(cm)	y_{PM}(cm)	z_{PM}(cm)
[1.6 : 1.2 : 6.4]	[1.6 : 1.2 : 4]	1.4

transition of the permanent magnet's remanent flux density from zero to its nominal value of 1.4T. The SC bulk above is then partially penetrated by the applied field, as shown in Fig. 2(b). To use the proposed equivalent-permeability model a 3D stationary ϕ-formulation can be used for all domains.

Parameter	YBCO	PM
n	21	-
E_0 [Vm^{-1}]	10^{-4}	-
J_{C0} [Am^{-2}]	1.82×10^8	-
B_0 [T]	0.1	-
B_{remanent} [T]	-	1.4

B. Computing the Distributed Equivalent-Permeability Values

The varying and distributed equivalent-permeability model considers different permeability values on different volume sections of the HTS bulk. Using the final result in Fig.2(b), the volume closest to the permanent magnet and the SC region with the highest magnetic field variation inside the superconductor will be sectioned into smaller volumes, as shown in Fig. 3(a). Also, due to the higher distance to the PM, the SC volume with lower magnetic field variation is kept as a single bulk since its field is mostly homogeneous.

Obtaining the equivalent-permeability values always requires an initial step where previous knowledge of the magnetic field inside each SC's volumes and its associated air volume is demanded. Figure 3(b) shows the magnetic flux density distribution when the SC volume is filled with air. On the contrary, Fig. 3(c) shows the magnetic flux distribution when the volume is now the YBCO bulk. Seeing the field distribution inside the superconductor (Fig. 3(c)), it is clear that the magnetic permeabilities will not be uniform along the bulk. The regions closest to the PM will have field penetration and, therefore, a higher valued permeability than the SC's upper region. Taking the modulus of the field components at each mesh point inside the superconductor $||\mathbf{H_{sc}}||$, and in the same point for the air volume $||\mathbf{H_a}||$, allows the elaboration of an equivalent-permeability surface map using (5). Of course, this process would most likely allow an accurate field representation inside the superconductor when represented by its equivalent-permeability model. However, using each mesh point would also introduce a level of complexity that is not the idea of the explored equivalent-permeability SC model. Hence, the approach consisted of dividing the SC into smaller parts, as shown in Fig. 3(a), and applying different but isotropic equivalent-permeability values to each volume section.

IV. THE INITIALIZATION PROCESS

To initialize the equivalent-permeability model, time-dependent E-J power law simulations are required. Considering the range and steps of each geometrical parameter shown in Table I, a total of 1800 simulations would be necessary to cover all possible geometries. However, it was verified that this initialization could be done using only a few FEA time-dependent simulations while maintaining high accuracy in force calculation.

In this study, the initial values of the equivalent SC model were made by selecting six different geometric configurations of the PM/SC system, all using the E-J power law SC model in an $H-$formulation time-dependent FEM simulation. The six geometries correspond to the combinations shown in Table III.

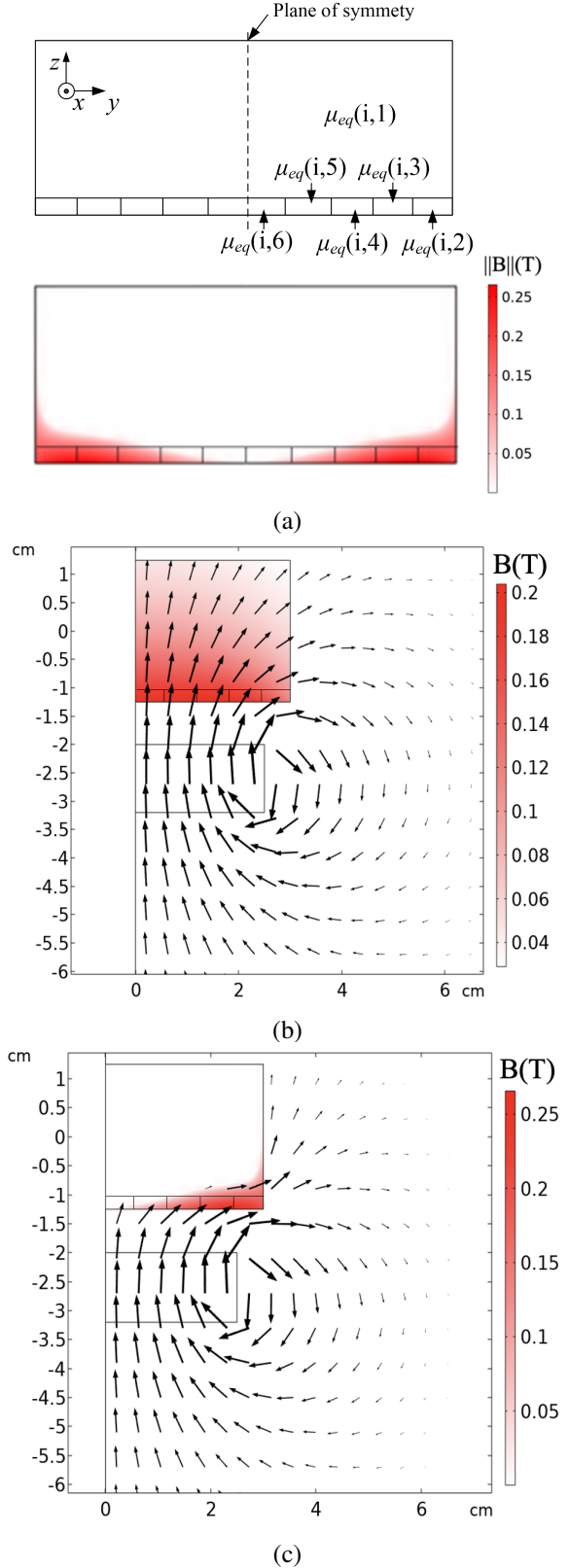

Fig. 3. (a) Distributed equivalent-permeability model representation for a certain simulation number i, where $\mu_{eq}(i,n)$ is the equivalent permeability of the ith simulation, determined in the nth block of the superconductor. (b) Magnetic flux density distribution when the volume occupied by the superconductor is considered filled with air, and (c) when the volume is the YBCO bulk.

TABLE III
SIX PM/SC GEOMETRIES USED FOR INITIALIZATION OF THE
EQUIVALENT-PERMEABILITY SC MODEL.

(1)	x_{SCmin}	y_{SCmin}	z_{SCmin}
(2)	x_{SCmin}	$0.44(y_{SCmax})$	z_{SCmin}
(3)	x_{SCmin}	$0.44(y_{SCmax})$	$0.44(z_{SCmax})$
(4)	x_{SCmin}	y_{SCmax}	z_{SCmax}
(5)	$0.44(x_{SCmax})$	y_{SCmax}	z_{SCmax}
(6)	x_{SCmax}	y_{SCmax}	z_{SCmax}
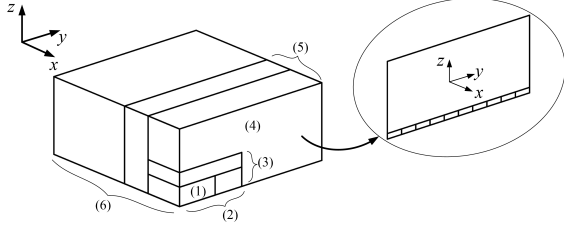
Fig. 4. Different HTS geometries present in Table III.

Fig. 5. Permeability values μ_{eq} for different values of applied magnetic field. In black for large block 1 and red for the small block 2 shown in Fig. 3a.

TABLE IV
AVERAGE TIME FOR ONE SIMULATION WITH BOTH SC MODELS (E-J
POWER LAW MODEL AND THE EQUIVALENT-PERMEABILITY MODEL) IN
THE FEM PROGRAM.

	E-J power law model	Permeability model
Computing time (s)	300 (5 min)	4

They cover the minimum and maximum dimensions of the SC geometry and some additional intermediary points. Notice that, as opposed to the research in [20] where the initialization was performed for all different geometries, we aim to prove that the initialization can be made using only a restricted number of FEM simulations. For this, a large-scale optimization was developed, as will be shown later.

A. Varying and distributed equivalent-permeability model

The initialization process of the PM/SC system in Fig. 2 uses the six different geometries listed in Table III. Combination (1) begins with the minimum dimensions for the SC bulk: x_{SCmin}, y_{SCmin}, and z_{SCmin}. We considered a step of $0.44x_{SC_max}$, $0.44y_{SC_max}$ and $0.44z_{SC_max}$ due to the even numbers of steps in Table I, and to be as close as possible to 50% of each variable. From (1) to (4), the area $y_{SC} \times z_{SC}$ is increased to increase the cross-sectional area of each discretization in Fig. 3(a), and finally x_{SC} is increased, which is the length of each discretization segment, Fig. 4. Figure 3(a) shows how the SC bulk is first divided into several volume sections, whose number and dimensions are set according to its magnetic flux distribution. Due to the symmetry of the SC/PM setup, in Fig.3(b) and (c), only the right side of the SC/PM symmetry axis is shown.

To exemplify the initialization process, consider two volumes in Fig. 3(a): block 1 with $\mu_{eq}(i,1)$, and the small block 2 with $\mu_{eq}(i,2)$. For each block, one begins calculating the equivalent-permeability value in each mesh element belonging to the block using (5). The volume of the associated mesh weights the equivalent-permeability value. Doing this for all element meshes belonging to the block, and summing all values, the equivalent-permeability value μ_{eq} of the block is then computed by dividing the sum result by the block volume. Figure 5 shows the evolution of the equivalent-permeability values to blocks 1 and 2 (black for block 1 and red for block 2) as one proceeds with the geometries' sequence of Table III from (1) to (6). As shown in Fig. 5, higher values of applied magnetic field lead at the end to higher equivalent-permeability

values. This is due to the lower capability of repelling the magnetic field when the applied magnetic field is higher. For example, the smaller divisions of the HTS bulk near the PM (block 2 with red results in Fig. 5) experience higher magnetic fields, thus, resulting in higher equivalent-permeability values.

For the remaining and possible SC/PM geometries, each equivalent-permeability value to blocks 1 and 2, for example, is obtained by first computing the applied magnetic field $||\mathbf{H_a}||$ in the HTS volume when this is not magnetized, using a stationary FEM simulation. Follow, the interpolated curve in Fig. 5 will give us the equivalent μ_{eq} for the previous applied magnetic field $||\mathbf{H_a}||$. Doing this for all blocks, a new stationary simulation is carried out to calculate the levitation force finally.

Table IV presents the average simulation time in seconds taken by a single simulation of each model of the six different geometric cases. Remember that a time-varying FEA was used in each simulation with the E-J power law model. Notice that this is an average time and not the time for every simulation. A time-varying simulation using the E-J power law can take about 30 minutes to complete, but the average value associated with the 6 geometries was about 5 minutes. On the other hand, using the equivalent-permeability model instead, the average simulation time was only 4 seconds using now a stationary FEA. After repeating the previous initialization process for the remaining blocks partitioning the SC volume, one obtains its associated permeability function for each block, as illustrated in Fig. 5.

Remember our PM/SC system and its geometric and multi-objective optimization problem (maximizing the force but minimizing the SC volume). In this framework, the question is, what is the advantage of using the equivalent-permeability model? Considering the range and steps of geometrical param-

Step	Single computational time	number	Total time
1	5 min	6 geometries	30 min
2	< 1s	1 computation	< 1s
3.1	4s	1800 sim	2 hrs
3.2	< 1s	1800 sims	< 1s
3.3	4s	1800 sims	2 hrs

TABLE VI
AVERAGE TIME FOR THE INITIALIZATION AND CONSTANT
EQUIVALENT-PERMEABILITY MODEL APPLICATION.

Step	Single computational time	number	Total time
1	5 min	1 sim	5 min
2	4s	1800 sim	2 hrs

eters listed in Table I, a total of 1800 configurations would be required to cover all possible geometries. Hence, the following steps would be required to use the equivalent-permeability model for every 1800 geometries.

1) Initialization of the μ_{eq} curves using different geometries (in our example, demands 6 time-dependent FEA E-J power law simulations);
2) Equivalent-permeability curves and its interpolation to obtain the μ_{eq} versus applied magnetic field;
3) For each one of the 1800 geometries, perform a stationary FEA simulation consisting in:
   3.1) stationary FEA simulation replacing the HTS bulk volume by air to compute the applied field $\|\mathbf{H_a}\|$ distribution in that volume;
   3.2) compute the μ_{eq} for each block of the HTS bulk using the μ_{eq} versus applied magnetic field from step 2);
   3.3) FEA SC/PM simulation using the μ_{eq} to obtain the levitation forces.

The computational time taken by each step is shown in Table V. Steps 1, 3.1, and 3.3 are critical regarding the total computational time. In the case of our SC/PM system, it took about 4.5 hours for the initialization and the equivalent-permeability model. However, if all 1800 simulations were carried out using the time-dependent E-J power law to represent the SC bulk at each optimization step, the resulting time would have been around 150 hours. Therefore, considering the initialization stage, the proposed methodology based on an equivalent-permeability SC bulk model allows a significant reduction of 97% of the computational time needed for an optimization process. Of course, the simulation time will depend on the hardware used. However, considering that the same hardware is used for all simulations needed, it is accurate enough to conclude that the equivalent-permeability model, especially if thousands of simulations are being done, such as for geometric and cost-wise optimizations, is much more time-efficient. Besides, it also has the advantage of being easily applied, not requiring extensive computations, and still finding the maximizing geometry.

B. Constant and distributed equivalent-permeability model

It is pertinent to analyze the option where the distributed equivalent-permeability model is initialized only once instead of using the six simulations shown in Table III. Let us refer to this as the constant equivalent-permeability model.

With a unique set of equivalent-permeability values for each sectioned bulk volume, all other geometries will consider the same distribution of the permeability values. We used the first calculated set of permeability values, which is the set corresponding to the first geometric combination with x_{PM}=1.60 cm, y_{PM}=1.60 cm, x_{SC}= 1.60 cm, y_{SC}=1.60 cm and z_{SC}= 0.7 cm. The procedure can be summarized in two steps:

1) Initialization of the μ_{eq} values using one geometry (1st), and;
2) For each geometry, perform a stationary simulation with the μ_{eq} values and obtain the levitation forces.

Table VI shows that the total optimization time took 2 hours and 5 min, while initialization based on the 6 geometries and variable μ_{eq}, the total optimization time was 4.5 hours. Remember that using the E-J power law takes a total computing time of 150 hours.

This approach also reduces computation time since the initialization is made using only one time-dependent simulation with the E-J power law to access the permeability values. Compared with the varying and equivalent-permeability model, this one takes about 1/6 of the time. Compared with optimization by applying the E-J power law to thousands of simulations, its computing time is negligible. However, using constant μ_{eq} values, it is assumed that the superconductor's magnetization does not change. For this reason, this approach should lead to a lower accuracy on the levitation force values. Hence, it is advisable to use it only in cases where the magnetic field distribution inside the HTS bulks is similar throughout all parametric variations.

C. Initialization results and accuracy

To analyze the accuracy of the variable distributed equivalent-permeability model and its initialization process, its results are compared with those obtained from 3D FEM simulations using the E-J power law model. The most important accuracy factor in optimization problems is not the direct error between force computation using the E-J power law and the value obtained using the equivalent-permeability model. Instead, it is more practical to verify if the model provides accurate results in finding the geometric configuration that maximizes the levitation force and minimizes the SC volume or, as we will name it, the force-maximizing geometric configuration. Of course, this geometric configuration must be the same using any model.

The accuracy of that process is computed using (6). In (6), A_{RM} stands for the accuracy with which we find the relative maximum in one of the equivalent-permeability models when
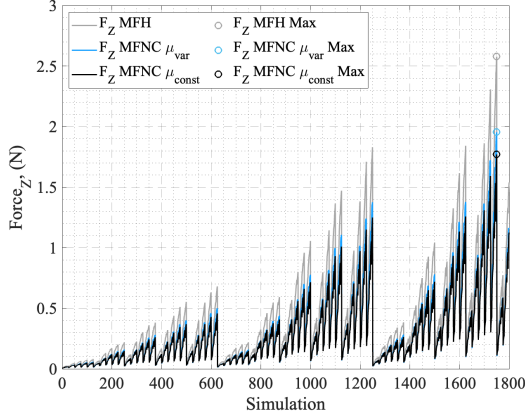
Fig. 6. Levitation force values F_z(N) for different geometric parameters in three models: E-J power law model (gray), variable permeability (blue), constant permeability (black), and respective global maximum force (circled).

TABLE VII
MAXIMUM GLOBAL LEVITATION FORCE VALUES, RESPECTIVE INDEXES, AND ACCURACY VALUES FOR MAXIMUM RELATIVE COMPUTATION A_{RM}.

	n	Fz^{Max}(N)	A_{RM}(%)
E-J model	1750	2.58	100
$\mu_{var} model$	1750	1.95	98.4
$\mu_{const} model$	1750	1.77	97.4

the reference is the E-J power law model. I_{EJH} and I_{SEPM} are the indexes of simulations using, respectively, the E-J power law plus the $H-$formulation (I_{EJH}) or using the constant equivalent-permeability model. I_n is the final index, the value of the total number of simulations performed. In I_{EJH}, term EJH corresponds to the 1800 time-dependent simulations with the E-J power law. In I_{SEPM}, term $SEPM$ corresponds to the constant equivalent-permeability model.

$$A_{RM} = 1 - \frac{|I_{EJH} - I_{SEPM}|}{I_n} \qquad (6)$$

Figure 6 shows for each n simulation-based optimization the levitation force values $Force_Z$ (N) using the E-J model (gray), the varying equivalent-permeability model μ_{var} in blue, or using the constant equivalent-permeability model μ_{var} plotted in black. The maximum force values obtained for each model are circled in Fig. 6, with their values listed in Table VII. This shows the indexes n corresponding to each model's geometry corresponding to a global maximum of the levitation force for the SC/PM system F_z^{Max}, also showing the accuracy factor from (6), A_{RM}.

In Table VII, by comparing the force values, the deviation between the varying and constant equivalent-permeability models are verified to be -24.4% and -31.4%, respectively, from the E-J model value. However, these results do not devalue the use of SC bulk models based on equivalent-permeability in an optimization process. Firstly, it is visible in Fig. 6 that the force function's overall monotony is identical for the time-dependent E-J power law model and both equivalent-permeability models throughout the entirety
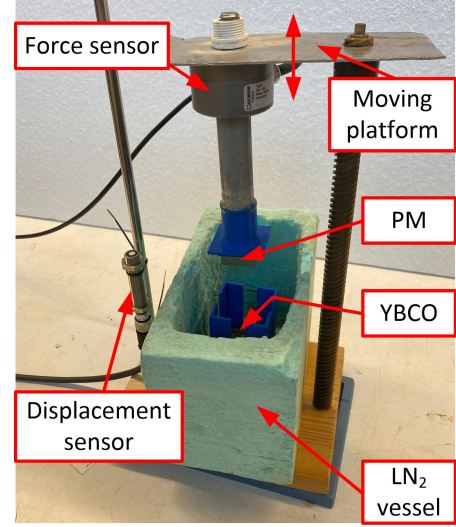
Fig. 7. Experimental setup for Levitation force measurements

of the SC/PM geometric parameters change. Secondly, since the superconductor and the permanent magnet sizes change iteratively, it can be assumed that it does not make a difference in the accuracy of the model, whether the geometric change is done on the permanent magnet or the superconductor. This is a very good indicator of the precision of the equivalent-permeability models for optimization purposes. Even with different maximum force values, the main goal, which is to find the optimal geometry, is still achieved with accuracy. The maximum force value can then be confirmed by experimenting or, with proximity, an E-J power law simulation.

Another very important fact to notice is that even though the accuracy of the relative maximum finding is not 100%, the global maximum of the force is found in all three models for the same geometric combination. Therefore, results show that the equivalent-permeability model can be used in the pre-design phase of bulk superconducting electromechanical devices, where a preliminary geometry must be first selected for further optimization.

V. EXPERIMENTAL VERIFICATION AND VALIDATION

Finally, to validate the model's accuracy and test different values of airgap, i.e., outside the initialization range, experimental tests (Fig. 7) were carried out in our lab with two different YBCO bulks at different distances from the PM. The superconducting bulks were chosen with two physical dimensions: 3.2x3.2x1.5 cm and 4x4x1cm, Fig. 8. The NdFeB permanent magnet used for both experiments had 2.54x2.54x1.28cm and a remanent magnetic flux density under liquid nitrogen of about 1.4T. A displacement sensor measured the vertical distance between the bulk and the permanent magnet. A force sensor was also installed above the permanent magnet to measure the levitation forces.

Figures 9 and 10 show the experimental and simulation results obtained using the E-J model and the varying and dis-
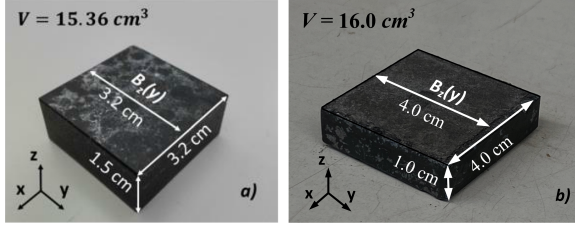
Fig. 8. HTS bulks used for experimental tests: a) 3.2 x 3.2 x 1.5 cm and b) 4.0 x 4.0 x 1.0 cm

tributed equivalent-permeability model. Based on the results, the equivalent-permeability model is validated by showing the same variability and similar results in force calculation as both the time-dependent E-J FEA model and the experimental values. This result is in good agreement with the previously obtained in section IV. The highest deviations are found for very small airgap since these are very far from the reference airgap of 3 cm used during the model's initialization. The obtained results, compared with experiments, confirm that the equivalent-permeability model continues to allow significant advantages for a pre-design process of electromechanical systems with HTS bulks. The fast computational time and good accuracy allow their incorporation in multi-objective/multi-constraints optimizations.
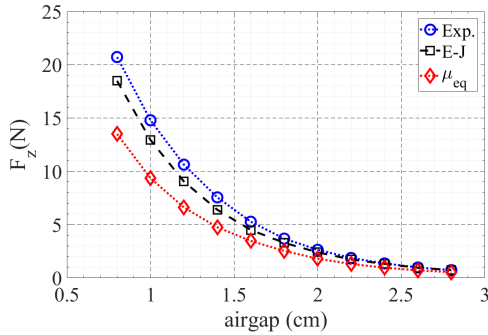
Fig. 9. Experimental, E-J and equivalent permeability levitation force values F_z(N) for YBCO bulk of 3.2x3.2x1.5cm
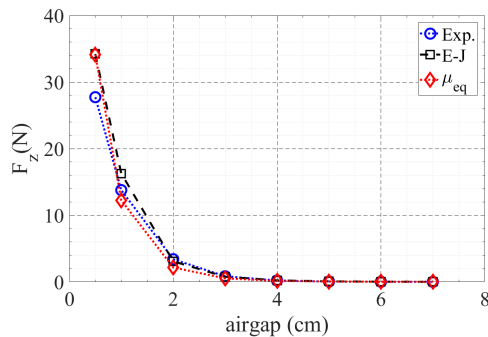
Fig. 10. Experimental, E-J and equivalent permeability levitation force values F_z(N) for YBCO bulk of 4x4x1cm
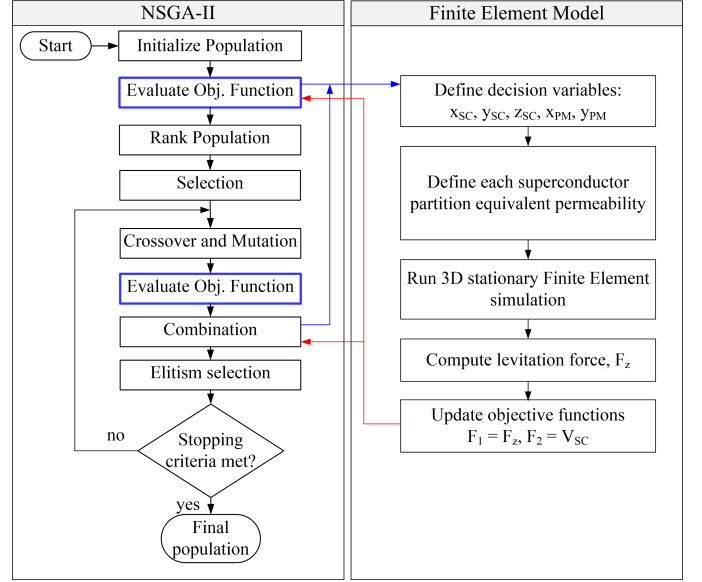
Fig. 11. Flowchart of the optimization problem.

VI. MULTI-OBJECTIVE OPTIMIZATION BASED ON EQUIVALENT-PERMEABILITY MODEL

In this section, a multi-objective optimization is carried out to optimize the levitation system shown in Fig. 2. The objective is to analyze the potential of using the equivalent-permeability model initialized using the six E-J time-dependent simulations (as described in Sections III and IV) in the pre-design of an electromechanical HTS bulk system.

The non-dominated sorting genetic algorithm II (NSGA-II) is used for multi-objective optimization [23]. This algorithm is a multi-objective, multi-constraint optimization tool based on the evolution of the population's genetic code, capable of providing a Pareto front with optimal solutions. Figure 11 shows a flowchart of the optimization process where the NSGA-II algorithm is combined with the equivalent-permeability model.

The multi-objective optimization problem is described by two objective functions, maximizing the levitation force, F_z, while minimizing the HTS bulk volume, V_{SC}, as described in (7). Please note that these two objective functions are contradictory because decreasing the volume of SC will ultimately decrease the levitation forces. Therefore, the final optimized solution will be a 2D Pareto front, instead of a single optimized point.

$$f = \{max(f_1 = F_z), min(f_2 = V_{SC})\} \qquad (7)$$

The decision variables, which will be optimized, are composed of the SC geometry and the PM's width and length. These variables are limited to their minimum and maximum sizes as described in Table VIII.

The optimization was performed with a population of 50 elements and 50 generations, resulting in 2500 different geometries tested. Fig. 12(a) shows the final Pareto front obtained after 3.5 hours, using the equivalent-permeability model in the FEA simulations. If the time-dependent E-J power law were

TABLE VIII
DECISION VARIABLES RANGE [CM].

SC width, x_{SC}	[1.225 2.8]
SC length, y_{SC}	[1.6 6.4]
SC height, z_{SC}	[1.6 6.4]
PM width, x_{PM}	[1.6 6.4]
PM length, y_{PM}	[1.6 4]

used in the FEA simulations, this would otherwise require around 208 hours (50×50×5min).

From the optimal Pareto front in Fig. 12(a), the designer can thus select the desired levitation force or superconductor volume to begin the system's design. Figures 12(b-f) show the evolution of variables x_{SC}, y_{SC}, z_{SC}, x_{PM}, and y_{PM}, all as a function of the superconductor volume, V_{SC}. The dashed red lines indicate the maximum range taken for each size. Besides providing information about the optimal solution for each levitation force (or SC volume), they also indicate the importance of each size in the optimization problem. For example, the height of the superconductor (z_{SC} in Figure 12(d) only begins increasing after its width x_{SC} reaches the maximum allowed range, highlighting the importance of its length and width values.

To further validate the optimization process, 5 points were selected from the Pareto front plotted in Fig. 12(a). These were simulated now using the time-dependent E-J power law FEM model to obtain their levitation force, as shown in Figure 13. These results show that the shape of the Pareto front is preserved and that the maximum deviation between models is around 17%. Notice that this is coherent with the results presented in Fig. 6. Thus, the equivalent-permeability model can provide a good compromise between results accuracy for calculating levitation forces in superconducting bulk systems and computational and multi-objective optimization times.

VII. CONCLUSION

In this study, distributed equivalent permeability-based models are tested for the pre-design of electromechanical systems with HTS bulks. A levitation system made of a superconductor bulk and a permanent magnet is analyzed as a case study. The proposed distributed equivalent-permeability models present high accuracy in finding the geometric configuration that maximizes levitation force. These equivalent models' simulations, requiring a quick initialization process, are much faster than time-dependent H-formulations. The required initialization process for the distributed equivalent-permeability models was tested using only 6 time-dependent E-J FEA simulations. This initialization method proved sufficient to assure good accuracy while requiring a low initialization time.

The force values obtained from the distributed equivalent-permeability models are compared with the time-dependent E-J power law FEA model for 1800 different geometries of the levitation system. Based on the obtained results, it is evident that the equivalent-permeability models allow estimating the geometry with the highest levitation force.

Furthermore, to prove the advantage of using the distributed equivalent-permeability models and the initialization

Fig. 12. Optimization results: (a) Levitation forces, F_z, as a function of the SC volume, V_{SC}, (b) SC width, x_{SC}, (c) SC length, y_{SC}, (d) SC height, $z_{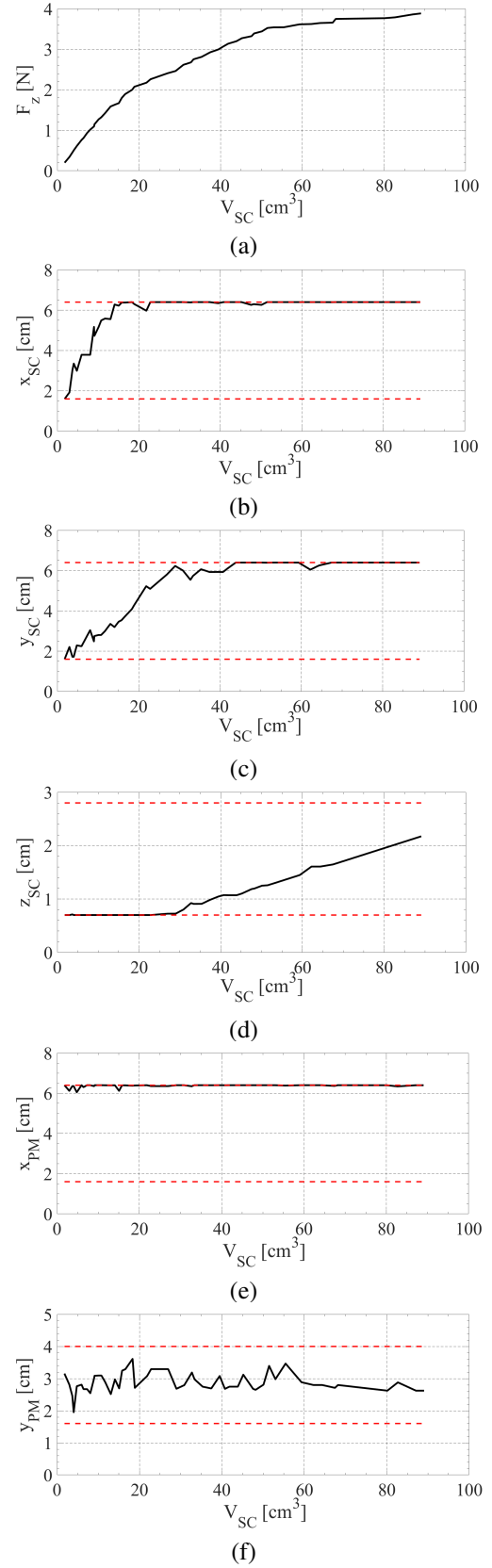SC}$, (e) PM width, x_{PM}, and (f) PM length, y_{PM}, as a function of the SC volume. In the dashed red line are the limits of each variable.

Fig. 13. Comparison between optimization results and FE E-J model. On the right axis is presented the deviation between curves.

process, a multi-objective optimization was performed based on the NSGA-II optimization tool to optimize the geometry of the levitation system. The final optimized results from the Pareto Front are very close to those obtained using the E-J $H-$formulation model. The total optimization time was 3.5h, while it would be required about 208h if the time-dependent E-J FEA model was used for the whole optimization process.

In addition, the model was experimentally validated using two YBCO bulks of different sizes and for different airgaps. Even with airgaps outside the range used for the model initialization, the equivalent permeability models present the same trend in levitation force values compared to the time-dependent E-J FEA and experimental results.

Therefore, as both equivalent models can predict the levitation forces, these have proven valuable for the pre-design optimization of electromechanical HTS systems, with a drastic time reduction.

REFERENCES

[1] J. Lloberas, A. Sumper, M. Sanmarti, and X. Granados, "A review of high temperature superconductors for offshore wind power synchronous generators," *Renewable Sustain. Energy Rev.*, vol. 38 pp. 404–414, 2014.
[2] X. Song et al., "Commissioning of the World's First Full-Scale MW-Class Superconducting Generator on a Direct Drive Wind Turbine," *IEEE Trans. Energy Convers.* vol. 35 pp. 1697-1704, Sept. 2020.
[3] T. Nakamura et al., "Tremendous Enhancement of Torque Density in HTS Induction/Synchronous Machine for Transportation Equipments," *IEEE Trans. Appl. Supercond.* vol. 25 pp. 1–4, June 2015.
[4] J. Sim, K. Lee, G. Cha and J. Lee, "Development of a HTS squirrel cage induction motor with HTS rotor bars," *IEEE Trans. Appl. Supercond.* vol. 14 pp. 916–919, June 2004.
[5] S. Baik, Y. Kwon, S. Park and H. Kim, "Performance Analysis of a Superconducting Motor for Higher Efficiency Design," *IEEE Trans. Appl. Supercond.* vol. 23 pp. 5202004-5202004, June 2013.
[6] U. Bong et al., "A Design Study on 40 MW Synchronous Motor With No-Insulation HTS Field Winding," *IEEE Trans. Appl. Supercond.* vol. 29 pp. 1–6, Aug. 2019.
[7] S. S. Kalsi, B. B. Gamble, G. Snitchler and S. O. Ige, "The status of HTS ship propulsion motor developments," in *Proc. IEEE Power Eng. Soc. Gen. Meet.*, 2006, pp.1-5.
[8] H. Moon et al., "An introduction to the design and fabrication progress of a megawatt class 2G HTS motor for the ship propulsion application," *Supercond. Sci. Technol.* vol. 29 no. 3, Feb. 2016.
[9] K. Kovalev, J. Nekrasova, N. Ivanov and S. Zhurzvlev, "Design of All-Superconducting Electrical Motor for Full Electric Aircraft," in *Int. Conf. Electrotechnical Complexes Syst. (ICOECS)*, 2019, pp. 1–5.
[10] P. J. Masson, M. Breschi, P. Tixador and C. A. Luongo, "Design of HTS Axial Flux Motor for Aircraft Propulsion," *IEEE Trans. Appl. Supercond.*, vol. 17 pp. 1533 – 1536, June 2007.
[11] J. Zheng, H. Huang, S. Zhang and Z. Deng, "A General Method to Simulate the Electromagnetic Characteristics of HTS Maglev Systems by Finite Element Software," *IEEE Trans. Appl. Supercond.* vol. 28 pp. 1–8, Aug. 2018.
[12] F. Sass et al., "$H-$formulation for simulating levitation forces acting on HTS bulks and stacks of 2G coated conductors," *Supercond. Sci. Technol.* vol. 28 no. 12, Nov. 2015, Art. no. 125012.
[13] M. Zhang and T.A. Coombs, "3D modeling of high-Tc superconductors by finite element software," *Supercond. Sci. Technol.* vol. 25, no. 01, Dec. 2011, Art. no. 015009.
[14] K. Yoshida, H. Matsumoto, "Propulsion and guidance simulation of HTS bulk linear synchronous motor taking into account E–J characteristic," *Physica C: Supercond.* vol. 392 - 396 pp. 690 – 695, 2003.
[15] F. Trillaud, K. Berger, B. Douine and J. Lévêque, "Comparison Between Modeling and Experimental Results of Magnetic Flux Trapped in YBCO Bulks," *IEEE Trans. Appl. Supercond.* vol. 26 pp. 1–5, April 2016.
[16] A. Arsenault, F. Sirois and F. Grilli, "Implementation of the H-ϕ Formulation in COMSOL Multiphysics for Simulating the Magnetization of Bulk Superconductors and Comparison With the $H-$Formulation," *IEEE Trans. Appl. Supercond.* vol. 31 pp. 1–11, March 2021.
[17] E. Berrospe-Juarez, V. M. Zermeno, F. Trillaud, and F.Grilli "Real-time simulation of large-scale HTS systems: multi-scale and homogeneous models using the T–A formulation," *Supercond. Sci. Technol.* vol. 32 no. 6, April 2019.
[18] B. Shen, F. Grilli and T. Coombs, "Review of the AC loss computation for HTS using H formulation," *Supercond. Sci. Technol.* vol. 33 no. 3, Feb. 2020.
[19] J. F. P. Fernandes, A. J. Arsenio Costa and J. Arnaud, "Optimization of a Horizontal Axis HTS ZFC Levitation Bearing Using Genetic Decision Algorithms Over Finite Element Results," *IEEE Trans. Appl. Supercond.* vol. 30 pp. 1–8, March 2020.
[20] I. S. P. Peixoto, F. F. da Silva, J. F. P. Fernandes and P. J. da Costa Branco, "3D Equivalent Space-Varying Permeability Model of HTS Bulks for Computation of Electromagnetic Forces," *IEEE Trans. Appl. Supercond.* vol. 31, no. 5 pp. 1–7, Aug. 2021.
[21] P. J. da Costa Branco and J. A. Dente, "Design and Experiment of a New Maglev Design Using Zero-Field-Cooled YBCO Superconductors," *IEEE Trans. Ind. Electron.* vol. 59 pp. 4120–4127, Nov. 2012.
[22] F. Ferreira da Silva and P. J. da Costa Branco, "Study of a cylindrical geometry design for a zero field cooled Maglev system," *Supercond. Sci. Technol.* vol. 32 no. 6, 2019.
[23] K. Deb et al., "A fast and elitist multiobjective genetic algorithm: NSGA-II," *IEEE Trans. on Evol. Comput.* vol. 6, pp. 182-197, 2002.